HAL
open science

Transverse and lateral confinement effects on the oscillations of a free cylinder in a viscous flow

Luciano Gianorio, Maria Veronica d'Angelo, Mario Cachile, Jean-Pierre Hulin, Harold Auradou

To cite this version:

Luciano Gianorio, Maria Veronica d'Angelo, Mario Cachile, Jean-Pierre Hulin, Harold Auradou. Transverse and lateral confinement effects on the oscillations of a free cylinder in a viscous flow. Physics of Fluids, 2014, 26 (084106), pp.1. 10.1063/1.4893342 . hal-00844311

HAL Id: hal-00844311

https://hal.science/hal-00844311v1

Submitted on 14 Jul 2013

HAL is a multi-disciplinary open access archive for the deposit and dissemination of scientific research documents, whether they are published or not. The documents may come from teaching and research institutions in France or abroad, or from public or private research centers.

L'archive ouverte pluridisciplinaire **HAL**, est destinée au dépôt et à la diffusion de documents scientifiques de niveau recherche, publiés ou non, émanant des établissements d'enseignement et de recherche français ou étrangers, des laboratoires publics ou privés.

Transverse and lateral confinement effects on the oscillations of a free cylinder in a viscous flow.

Luciano Gianorio,[a] Maria Veronica D'Angelo,[b] and Mario Cachile[c]
Grupo de Medios Porosos, Facultad de Ingeniería, Paseo Colon 850, 1063, Buenos Aires (Argentina), CONICET (Argentina).
Jean-Pierre Hulin[d] and Harold Auradou[e]
Univ Pierre et Marie Curie-Paris 6, Univ Paris-Sud, CNRS, F-91405. Lab FAST, Bât 502, Campus Univ, Orsay, F-91405 (France).

(Dated: July 14, 2013)

The different types of instabilities of free cylinders (diameter D, length L) have been studied in a viscous flow (velocity U) between parallel vertical walls of horizontal width W at a distance H: the influence of the confinement parameters D/H and L/W has been investigated. As D/H increases, there is a transition from stable flow to oscillations transverse to the walls and then to a fluttering motion with oscillations of the angle of the axis with respect to the horizontal. The two types of oscillations may be superimposed in the transition domain. The frequency f of the transverse oscillations is independent of the lateral confinement L/W in the range: $0.055 \leq L/W \leq 0.94$ for a given cylinder velocity V_{cx} and increases only weakly with V_{cx}. These results are accounted for by assuming a $2D$ local flow over the cylinder with a characteristic velocity independent of L/W for a given V_{cx} value. The experimental values of f are also independent of the transverse confinement D/H. The frequency f_f of the fluttering motion is significantly lower than f: f_f is also nearly independent of the cylinder diameter and of the flow velocity but decreases significantly as L/W increases. The fluttering instability is then rather a $3D$ phenomenon involving the full length of the cylinder and the clearance between its ends and the side walls.

I. INTRODUCTION

The transport of elongated particles or microorganisms by a confined flow is relevant to many industrial applications and natural phenomena. This is for instance the case in bioengineering or enhanced oil recovery processes or in the build-up and structuration of biofilms in flow channels. We are interested in the present work in the instabilities of the motion of single elongated particles (here cylinders) free to move in viscous flows. The characteristic dimensions of the particles are comparable to those of the section of the flow channels so that confinement influence very strongly their transport and the occurrence of instabilities. This study is therefore relevant for instance, to the transport of fibers or long bio-particles in micro-fluidic channels or in porous and fractured media.

Previous studies in such flow configurations dealt frequently with the prediction or measurement of the hydrodynamic forces on static cylinders submitted to a flow between parallel plates or in a rectangular channel[1–3]. Investigations of moving cylinders in such geometries were often restricted to stable motions[4–8]; studies of flow instabilities in these geometries dealt mostly with vortex shedding behind fixed cylinders between parallel walls[9–11]. Finally, instabilities occurring during the sedimentation of different types of objects in a viscous fluid were mostly analysed when no confinement effects were present[12,13]. Periodic fluttering-like motions have also been studied on plates falling in air, but also without considering the effect of confinement[14–16].

Regarding the present configuration, two previous papers reported experiments and $2D$ numerical simulations of the motion of a tethered[17] or free[18] horizontal cylinder of diameter D inside a parallelepiped Hele-Shaw cell where a vertical Poiseuille flow of velocity U is established. Transverse oscillations of the cylinder in the aperture H of the cell are observed both when the cylinder is tethered and when it can move freely across as well as in the plane of the cell. Moreover, in this latter case, the cylinder displays, in addition, oscillations of its rolling angle about its axis and of its vertical position at frequencies respectively equal to and twice that of the transverse oscillations. An important feature is that, in both cases, these oscillations have been observed at Reynolds numbers Re as low as 20: this is well below the threshold value generally reported by other authors for vortex shedding in confined geometries[19]. This suggests that one deals with a mechanism different from those associated to the destabilization of the wake of fixed bodies. The instability observed here cannot appear if the cylinder is fixed: it involves likely a feedback effect originating in the variations of the pressure and viscous forces induced by the motion of the cylinder.

In these previous studies the flow was either exactly (simulations)[17] or approximately (experiments)[18] two dimensional in the whole cell: in the experiments, the length L of the cylinder was indeed nearly equal to the width W of the cell (experiments) and only cases in which the cylinder remained horizontal were studied.

[a] Electronic mail: luchogiano@gmail.com
[b] Electronic mail: vdangelo@fi.uba.ar
[c] Electronic mail: mcachil@fi.uba.ar
[d] Electronic mail: hulin@fast.u-psud.fr
[e] Electronic mail: auradou@fast.u-psud.fr

The present work studies instead the influence of the length L ($< W$) on the instabilities; it also deals both with oscillations modes transverse to the cell aperture and with fluttering modes in which the cylinder does not remain horizontal.

After identifying the different flow regimes, one studies the influence of the ratio L/W on the instability over the range $0.055 \leq L/W \leq 0.94$: as L/W becomes smaller, the influence of the bypass flow between the ends of the cylinder and the sides of the cell becomes larger. Of special interest is the variation of the frequency f with the velocities V_{cx} and U of the cylinder and the flow and the relation between V_{cx} and U. Then, the influence of the blockage ratio D/H is investigated over the range of values: $0.39 \leq D/H \leq 0.77$. One studies finally the fluttering motion of the cylinder in the plane of the cell which appears at large values of D/H and/or L/W: the motion of the cylinder displays then periodic variations of the angle of the cylinder with respect to horizontal and oscillatory displacements parallel to its axis.

II. EXPERIMENTAL SETUP AND PROCEDURE

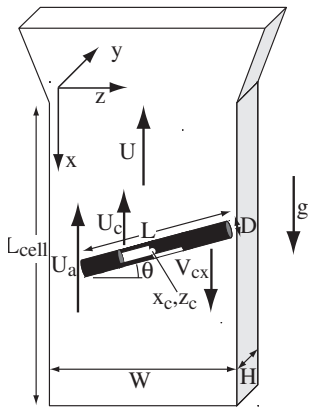

Figure 1. Schematic view of the experimental setup.

The experimental setup has been described in detail in ref. 18. The length L_{cell}, width W and aperture H of the Hele-Shaw cell (Fig. 1) are respectively equal to 290, 90 and 2.85 mm. The flowing fluid is a water-glycerol solution of concentration in weight $C = 10\%$. The viscosity and density of the solution at $T = 25^oC$ are respectively $\mu = 1.153$ mPa.s and $\rho_f = 1021\,\mathrm{kg/m^3}$. The flow rate varies between 0 and 400 ml/mn corresponding to mean velocities $-25 \leq U \leq 0$ mm/s (U is negative for an upward flow velocity since the vertical axis U is oriented downward). The top part of the cell as a Y-shape so that the local aperture increases from 2.85 to 6 mm over a vertical distance of 48 mm. All the experiments are performed using plexiglas cylinders of density $\rho_s = 1.19 \times 10^3\,\mathrm{kg/m^3}$. Their lengths range between 5 and 85 mm ($0.055 \leq L/W \leq 0.94$) and their diameter between 1.1 and 2.2 mm, ($0.39 \leq D/H \leq 0.77$).

At the beginning of the experiment the cylinders are placed horizontally at the top end of the cell and one lets them drift into the constant aperture region by reducing the flow rate Q; Q is then adjusted in order to bring the cylinder at the desired initial location and is kept constant thereafter during the measurements.

The displacement of the cylinder is monitored by a digital camera viewing the Hele Shaw cell from the front: its resolution is 1024×768 pixels and the frame rate 30 fps. In order to analyze the motion of the cylinder, its length is divided into 4 parts: the two outside ones are painted in black while black staggered stripes parallel to the axis are painted on the central portions. Processing digitally the images provides first the location of the ends of the cylinder by detecting the ends of the outer stripes: from these data one determines then the coordinates (x_c, z_c) of the center of mass of the cylinder and its angle θ with respect to the horizontal. As observed previously[18], oscillations of the cylinder transverse to the walls of the cell are accompanied by oscillations at the same frequency f of the angle of rotation of the cylinder about its axis: the variations of this angle are estimated by computing the transverse displacement of the staggered stripes painted on the cylinder with respect to those of the ends. The frequency of the oscillations is, here, deduced from the variation of this angle with time.

III. DIFFERENT CYLINDER MOTION REGIMES

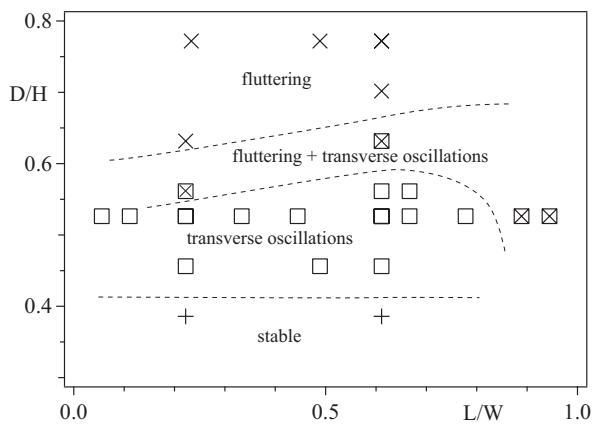

Figure 2. Different types of cylinder motions observed as a function of the ratios D/H and L/W for a plexiglas cylinder and a water-glycerol solution ($C = 10\%$): straight trajectory (+); transverse oscillation (□); fluttering+transverse oscillation (⊠); fluttering (×).

The different types of motion the free cylinder have been identified for different values of the control parameters D, L and U. The diameter and the length of the cylinder were observed to have the largest influence on the results: we have therefore displayed in Fig. 2 a map of the different regimes observed as a function of the dimensionless parameters D/H and L/W.

- For $D/H \lesssim 0.4$, the cylinder follow a straight stable vertical trajectory with no transverse or side oscillations.
- For higher ratios $0.4 \lesssim D/H \lesssim 0.6$, it displays transverse oscillations. When the length L becomes of the order of W ($L/W \gtrsim 0.9$), a fluttering motion is superimposed onto the transverse oscillations ($D/H = 0.53$): it corresponds to a periodic variation of the angle θ with the horizontal with a frequency significantly lower than that of the transverse oscillations.
- For $D/H \gtrsim 0.6$ a fluttering motion without transverse oscillation generally occurs except for $L/W = 0.61$, $D/H = 0.63$ in which case the two types of oscillations are again superimposed.

In short, increasing the ratio D/H and, therefore, the transverse confinement results in a transition from stable flow to transverse oscillations and then to a fluttering motion: moreover, fluttering appears earlier for strong longitudinal confinements.

IV. INFLUENCE OF THE CONFINEMENT ON THE TRANSVERSE OSCILLATIONS

A. Influence of the cylinder length

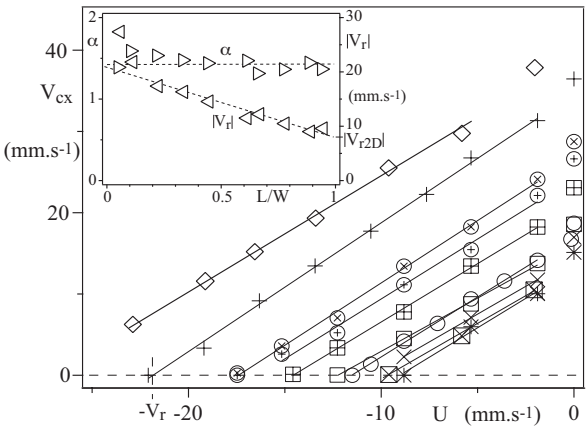

Figure 3. Influence of the length L of plexiglas cylinders of constant diameter $D = 1.5\,\mathrm{mm}$ ($D/H = 0.53$) on the variation of cylinder velocity V_{cx} with the velocity U of a flow of water with 10% glycerol. Symbols: experimental data; straight lines: linear regressions over these data (excluding point $U = 0$). $L/W = 0.055$ (◊), 0.11 (+), 0.22 (⊗), 0.33 (⊕), 0.44 (⊞), 0.61 (◯), 0.67 (□), 0.77 (×), 0.89 (∗) and 0.94 (⊠). Inset: variation as a function of the cylinder length L of the slope α of the linear regressions (▷) and of the velocity $|V_r|$ (◁).

The influence of the lateral confinement parameter L/W on the transverse oscillations has first been studied: experiments have been performed for free cylinders of diameter $D = 1.5\,\mathrm{mm}$ ($D/H = 0.53$) and L varying between 5 and 85 mm ($0.055 \leq L/W \leq 0.94$).

A first important characteristic is the variation of the velocity V_{cx} of the cylinder as a function of that of the flow (U) which is here oriented upward and, therefore, negative. The main graph in Fig. 3 shows that V_{cx} varies linearly with U (data points corresponding to $U = 0$ are however above the linear trend). For the curves of Fig. 3 corresponding to $L/W \leq 0.77$, only transverse oscillations occur: the axis of the cylinder remains horizontal and no flutter is visible. For $L/W = 0.89$ (∗) and $L/W = 0.94$ (⊠), the cylinder both flutters and oscillates transversally.

The straight lines on the main graph of Fig. 3 correspond to a linear regression on the data according to the equation:

$$V_{cx} = \alpha(U - V_r); \tag{1}$$

The variations with L/W of the slope $\alpha = \mathrm{d}V_{cx}/\mathrm{d}U$ of the regression lines and of V_r are plotted in the inset: α depends only weakly on L, even when fluttering occurs (▷ symbols) and its values are all in the range 1.4 ± 0.1. From Eq:1, V_r (< 0) is the velocity of the upward flow at which the cylinder remains at a constant average vertical position[18]; more generally V_r can be considered as a relative velocity of the fluid and the cylinder: the fact that it remains constant for a free cylinder as V_{cx} suggests that the drag force on the cylinder is determined by V_r and remains constant as V_{cx} varies for a given free cylinder in order to balance its weight. In contrast to α, $|V_r|$ decreases as L increases (◁ symbols): the limit of V_r as $L \to W$ corresponds to the value V_{r2D} for a $2D$ configuration with, here: $V_{r2D} = -9\,\mathrm{mm.s}^{-1}$. The slope of the variation of $|V_r|$ with L/W is almost constant except at the lowest values for which it increases sharply.

Fig. 4, displays the variation of the frequency f with the cylinder velocity V_{cx} for the different lengths L: one observes then an excellent collapse of the different curves onto a common weakly increasing trend, with, for $V_{cx} = 0$, a frequency $f = 3.3 \pm 0.1\,\mathrm{Hz}$. The data points are much more dispersed when f is plotted as a function of U (see inset).

We explain now the above result, namely that, for free cylinders, the frequency f is independent of L/W when the velocity V_{cx} is kept constant. When $L \to W$ (like in Ref. 18), flow is two dimensional with a zero bypass flow between the ends of the cylinder and the side walls. The balance, per unit length, between the weight of the cylinder and the vertical hydrodynamic force is then[3]:

$$\lambda_{p2D}\,\mu\,U - \lambda_{s2D}\,\mu\,V_{cx} = -(\rho_s - \rho_f)A\,g \tag{2}$$

(A is the cylinder section). Eq. (2) can then be rewritten in the form similar to Eq. (1):

$$V_{cx} = \frac{\lambda_{p2D}}{\lambda_{s2D}}U + \frac{(\rho_s - \rho_f)Ag}{\lambda_{s2D}\,\mu} = \alpha_{2D}(U - V_{r2D}), \tag{3}$$

in which V_{r2D} and α_{2D} are constant with U. V_{r2D} and α_{2D} will be equal to the limits of V_r and α when $L/W \to$

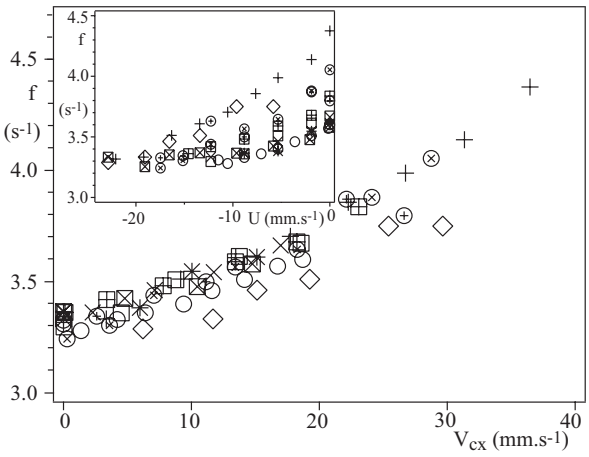

Figure 4. Experimental variation of the transverse oscillation frequency f as a function of the cylinder velocity V_{cx} for plexiglas cylinders of different dimensionless lengths L/W and constant dimensionless diameter $D/H = 0.53$. Inset : same frequency data as in the main graph plotted as a function of the mean flow velocity U. In both graphs, the symbols are the same as in Fig. 3.

1 with, for $D/H = 0.53$, from the inset of Fig. 3: $|V_{r2D}| = 9\,\mathrm{mm.s^{-1}}$ and $\alpha_{2D} = 1.4$

In the general case $L < W$, the local flow in the part of the aperture occupied by the cylinder is still assumed to be two dimensional: more precisely, one assumes that the velocity component v_z is negligible and that $v_x(x, y)$ and $v_y(x, y)$ are independent of z along the length L of the cylinder. The results to be discussed below suggest that this assumption is valid for $L/D \gtrsim 7$.

The balance of forces per unit length on the cylinder should then be the same as for $L = W$: Eqs. 2 and 3 remain then valid with the same parameters λ_{s2D} and λ_{p2D} (or V_{r2D} and α_{2D}) provided U is replaced by a local velocity U_{loc} constant along the length L. Then:

$$V_{cx} = \frac{\lambda_{p2D}}{\lambda_{s2D}} U_{loc} + \frac{(\rho_s - \rho_f)Ag}{\lambda_{s2D}\,\mu} = \alpha_{2D}(U_{loc} - V_{r2D}). \quad (4)$$

U_{loc} is related to V_{cx} and V_{r2D} by Eq. (4) and is, therefore, independent of L/W. Since the velocities U_{loc} and V_{cx} determine completely the local flow on the cylinder and, therefore, the frequency f, the latter will also be independent of L/W: this explains the excellent coincidence of the curves of Fig. 4.

In order to understand the relation between V_r and L/W displayed in the inset of Fig. 3, one estimates first the difference $U_{loc} - U$. The flow in each clearance of width $(L - W)/2$ between the ends of the cylinder and the sides of the cell (Fig. 1) is, like around the cylinder, assumed to be viscous and two dimensional: the corresponding velocity U_a averaged over the aperture H is then constant with z along its width $W - L$. Applying mass conservation, U, U_a and U_{loc} satisfy $U = (U_{loc}\,L + U_a\,(W - L))/W$. Moreover, the constant value of α, in particular as $L \to W$ allows one to take $\alpha = \alpha_{2D}$.

Combining these two latter results with Eqs. (1) and (4) leads then to:

$$V_r - V_{r2D} = U - U_{loc} = \frac{W - L}{W}(U_a - U_{loc}) \quad (5)$$

Taking for simplicity $V_{cx} = 0$, momentum conservation requires that the force due to the pressure drop Δp between the upstream and downstream sides of the cylinder balances its effective weight per unit length. Then: $\Delta p\,H = (\rho_s - \rho_f)Ag$ so that Δp is independent of L/W. Assuming a transverse pressure equilibrium, the pressure drop across the clearance between the cylinder and the walls must also be Δp. Under the above assumptions of a $2D$ viscous flow, the velocity U_a is proportional to Δp with a coefficient independent of the width $W - L$. Like Δp, U_a is then constant with L/W and Eq. (5) predicts the linear variation of V_r with L/W observed experimentally. Still for $V_{cx} = 0$ and $D/H = 0.53$ one has, from Eq. (4): $U_{loc} = V_{r2D} = -9\,\mathrm{mm.s^{-1}}$ (see above for the determination of V_{r2D}). Taking $L = 0$ in Eq. (5) leads then to: $U_a = V_r(L/W \to 0) = -27\,\mathrm{mm.s^{-1}}$.

B. Influence of the diameter on the transverse oscillations

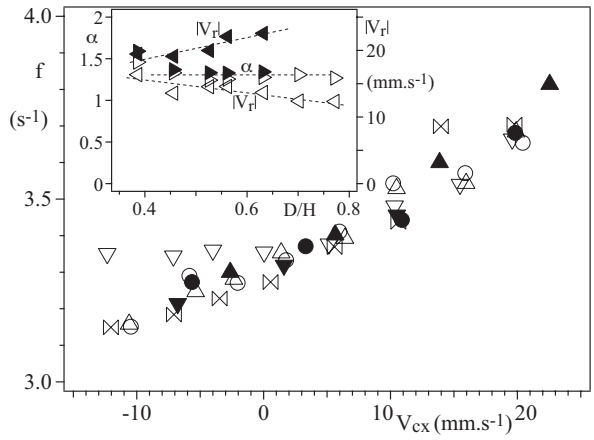

Figure 5. Experimental variation of the transverse oscillation frequency as a function of the mean flow velocity U for plexiglas cylinders of different diameter to aperture ratios: $D/H = 0.46$ (▽, ▼), 0.53 (◯, •), 0.56 (△, ▲), 0.63 (⋈). Open symbols: $L/W = 0.61$; black symbols: $L/W = 0.22$. Flowing fluid: water-glycerol solution ($C = 10\,\%$). Inset: variation of the slope α and the velocity V_r with the diameter D. Data points corresponding to $D/W = 0.39$ (stable regime), 0.7 and 0.77 (pure fluttering regime) have been added for comparison.

The influence of the transverse confinement parameter D/H on the transverse oscillations has been investigated by using several cylinders with different diameters and for two different lateral confinements ($L/W = 0.61$ and $L/W = 0.22$): the values of D/H belonged to the interval $0.39 \leq D/H \leq 0.77$. Transverse oscillations were observed in the range $0.46 \leq D/H \leq 0.63$.

The inset of Fig. 5 displays the variation of the parameters α and V_r with D/H: data points corresponding to pure fluttering ($D/H = 0.7$ and 0.77) or to stable ($D/H = 0.39$) regimes have also been included in this graph. The experimental value of α is independent of D/H with $\alpha = 1.34 \pm 0.1$ for both transverse confinement ratios L_c/W; moreover, the transition to the stable or fluttering regimes does not result in any variation of α.

The velocity V_r decreases smoothly by 30% as D/H varies from 0.39 to 0.77 for $L/W = 0.61$ and increases by 15% as D/H varies from 0.39 to 0.63 for $L/W = 0.22$: like for α, there is no visible influence of the transition from a flow regime to another.

The variation of the oscillation frequency with the cylinder velocity V_{cx} is plotted in the main graph of Fig. 5 for these same cylinders. All data points correspond to pure transverse oscillations except for $L/W = 0.61$ and $D/H = 0.63$ (Fig. 2): in this latter case, transverse oscillations and fluttering occur simultaneously. The frequency f is also remarkably independent of the ratio D/H for all values of D/H, except for the smallest diameter $D/H = 0.46$ and for $L/W = 0.61$: in this particular case, the common trend of variation of f with V_{cx} is only followed for $V_{cx} > 0$. but the values of f are higher for $V_{cx} \leq 0$. No special feature of the variations is observable when fluttering is superimposed onto transverse oscillations. The curves corresponding to the two different values of L/W (0.22 and 0.61) also coincide which generalizes the results obtained for $D/H = 0.53$ and displayed in Fig. 4.

V. FLUTTERING OSCILLATIONS OF THE CYLINDER

The fluttering instability is characterized by oscillations of the angle θ of the axis of the cylinder with respect to the horizontal (Fig. 6a) and dashed line in Fig. 6b. These angular oscillations are accompanied by synchronous variations of the lateral displacement δz_c of the center of mass (continuous line): the angle $|\theta|$ reaches an extremal value shortly after the end of the cylinder is closest to one of the sides of the cell.

The fluttering motion also induces fluctuations of the vertical velocity v_x of the cylinder. These variations are visualized in the figure (dotted line) from the deviation δx_c of the vertical coordinate from the linear trend which would correspond to a constant velocity: δx_c oscillates at twice the fluttering frequency indicating that negative and positive deviations of the angle θ have the same influence on the velocity. In the transverse oscillations regime, vertical oscillations at a frequency $2f$ have also been observed although, in this case, the cylinder remained horizontal[18].

Fig. 7 displays variations of the fluttering frequency f_f as a function of the velocity V_{cx} or the lateral confinement L/W for different pairs of values of the ratios L/W and D/H. As mentioned above, the fluttering instability is

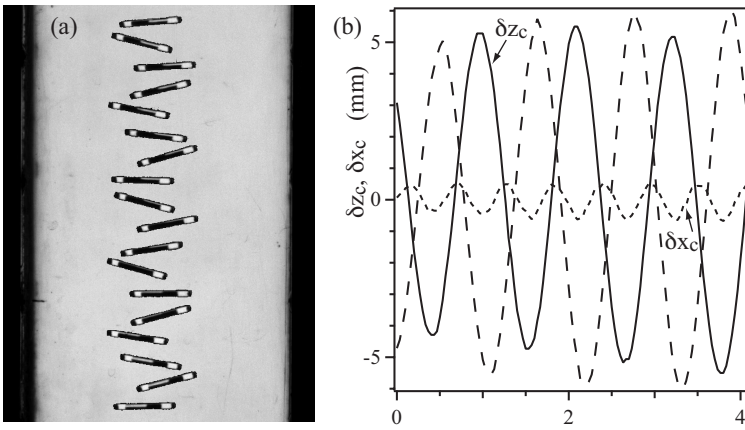

Figure 6. a) Successive views of the cylinder taken at time intervals $\Delta t = 1/3\,\mathrm{s}$ in the fluttering regime. b) Variations as a function of time in the same experiment of the geometrical parameters characterizing the motion of the cylinder in the fluttering regime; δz_c: distance from the vertical axis of symmetry of the cell (continuous line), δx_c: deviation of the vertical coordinate from a linear variation with time (dotted line), θ: angle of the axis with respect to the horizontal (dashed line). $L/W = 0.22$, $D/H = 0.63$, $U = 6.6\,\mathrm{mm.s}^1$.

observed for large values of $D/H \geq 0.63$ either alone or superimposed onto transverse oscillations (see Fig. 2). For $D/H = 0.53$, fluttering is only observed (together with transverse oscillations) for the largest ratios $L/W \geq 0.89$.

A first specific feature of this instability is that the frequency f_f is more than 3 times lower than that of the transverse oscillations; f_f decreases significantly with L/W, *e.g.* by a factor 3 as L/W increases from 0.22 to 0.9 (main graph of Fig. 7).

The strong influence of L/W on f_f suggests that these oscillations are driven by the dissymmetry between the bypass flows at the two ends of the cylinders when it moves laterally ($\delta z_c \neq 0$): the forces at the two ends of the cylinder are then unequal, which creates a torque that rotates it and a lateral force inducing a sideways motion.

Finally, for a given cylinder, f_f is independent of the velocity V_{cx} (and on U, too) as can be seen in the upper inset of Fig. 7. In this same graph, ones observes that the frequencies f_f corresponding to the same ratio $L/W = 0.61$ and to different values of D/H (0.63, 0.7, 0.77) coincide at all velocities ((◯), (⊕ and (⊗) symbols). Similarly, in the main graph, for $L/W = 0.22$, the values of f_f corresponding to $D/H = 0.63$ and 0.77 are nearly equal.

Regarding the mean vertical velocity V_{cx}, the slope α of the variation with U is practically independent of L/W (insert at lower left of Fig. 3): the common value is the same as that found previously in the stable and transverse oscillation regimes (insert of Fig. 3) Also, like in the case of transverse oscillations, the velocity $|V_r|$ decreases significantly as the ratio L/W increases; the

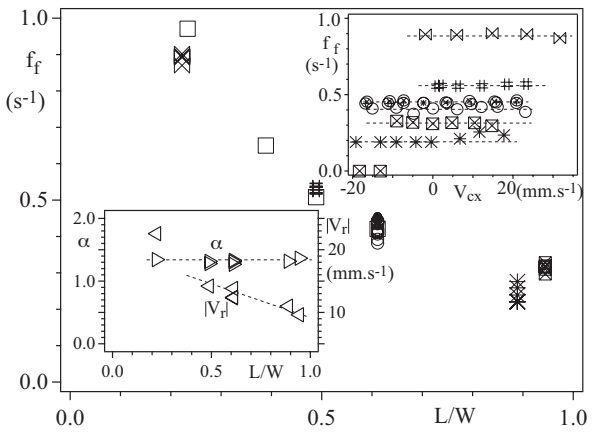

Figure 7. Experimental variation of the fluttering frequency f_f for a water-glycerol solution ($C = 10\,\%$) as a function of the normalised length L/W for plexiglas cylinders. Inset at lower left: variation of the slope α ($\triangleright$) and the velocity V_r ($\triangleleft$) with L/W for different diameters ($0.53 \leq D/H \leq 0.77$). Inset at upper right: variation of f_f with V_{cx} for cylinders with different values of D/H and L/W ($f = 0$ means: no oscillation). Dimensionless length and diameter of the cylinders: $D/H = 0.63$, $L/W = 0.22$ ($\bowtie$); $D/H = 0.77$, $0.22 \leq L/W \leq 0.61$ ($\square$); $D/H = 0.77$, $L/W = 0.49$ (#); $D/H = 0.53$, $L/W = 0.89$ ($*$); $D/H = 0.53$, $L/W = 0.94$ ($\boxtimes$); $D/H = 0.63$, $L/W = 0.61$ ($\bigcirc$); $D/H = 0.7$, $L/W = 0.61$ ($\oplus$);$D/H = 0.77$, $L/W = 0.61$ ($\otimes$)

value of V_r is also nearly independent of D/H.

At a first glance, these fluttering instabilities have visual similarities with those observed for falling sheets (or leaves)[14–16]: these latter experiments are however realized in unconfined configurations. These instabilities, which take place in unconfined configurations, take however place at larger Reynolds numbers: they involve vortex shedding from the edges of the sheets in contrast with the present ones.

VI. CONCLUSION

The present experiments demonstrate that the motion of a buoyant cylinder in a vertical viscous Hele Shaw cell flow may display oscillatory transverse and/or fluttering instabilities depending on the value of the two confinement parameters L/W and D/H. For $0.2 \leq L/W \leq 0.8$, for instance, one shifts continuously from the stable regime to the transverse oscillations and then to fluttering as D/H increases; at the transition, the two oscillatory instabilities may, in addition, be superimposed. These instabilities are controled by the relative velocity between the fiber and the fluid. They are observed for Reynolds numbers (based on the relative velocity) as low as 20: the mechanisms of the instabilities are thus different from those associated to destabilization of the wake at the rear of a fiber.

In an approximate description, the transverse instability is considered as a $2D$ one, corresponding to a local relative velocity with the same value V_{r2D} as for a cylinder of length $L = W$ (the transverse deviations of the flow lines are neglected). V_{r2D} is determined by the cylinder velocity V_{cx} and a local flow velocity U_{loc}. Both V_{r2D} and U_{loc} cannot be determined directly with the present setup: they can however be assumed to be equal respectively to the experimental values of V_r and U in the limiting case $L/W \to 1$. As a result, the frequency f is independent of L/W for a constant velocity V_{cx} (but depends instead on L/W for a constant velocity U); also, f increases by less than 15% when V_{cx} varies from 0 to $20\,\mathrm{mm.s}^{-1}$ in agreement with the results report in[18]. This $2D$ description is not valid for the shortest cylinders ($L/W = 0.055$) of aspect ratio $L/D = 1.75$.

The above discussion is only valid for free cylinders. For tethered ones[17] for which $V_{cx} = 0$, there is no longer an equilibrium between the hydrodynamic forces on the cylinder and its weight because of the tension of the supporting threads. In this case, the frequency f depends both on U and on L/W: f is indeed determined in this case by the local velocity U_{loc}. If the fiber and the fluid have the same density (this situation was considered by Berthet[20]), we have $V_{cx} = \alpha U$, and a relative velocity $V_r = 0$. In this case, fluttering and oscillations in the gap will not be observed.

Reverting to the free case, the frequency $f(V_{cx})$ is also found experimentally to be independent of the dimensionless diameter D/H: this result is quite surprising since, a first view, several mechanisms might induce a variation of f. Due to the lack of dependence of f on L/W, one can consider this problem for simplicity in the $2D$ case equivalent to $L/W = 1$. First, increasing D/H increases the section and, therefore, the mass of the cylinder which should reduce the frequency f. Increasing D also reduces the clearance $H - D$ and enhances the velocity (and Bernoulli pressure) variations: this should instead increase the value of f. Varying D also influences the relative velocity V_{r2D} and, as a result: f. Increasing D increases first the weight of the cylinder which is the driving force in Eq. (2); it should also increase the drag by reducing the clearance between the cylinder and the front walls. These two effects will respectively tend to increase and reduce the relative velocity (and therefore the frequency). $2D$ numerical simulations should allow one to determine the relative magnitude of the different effects and whether they compensate each other.

In contrast, the fluttering instability is strongly related to the variations of the distances between the ends of the cylinder and the sides of the cell: understanding it requires a model at the scale of the full width W of the Hele Shaw cell.

In spite of these differences, the transverse and fluttering instabilities of free cylinders share several common properties. Both f and f_f depend weakly, or not at all, on the velocity V_{cx} for a given cylinder: in both cases, this results from the fact that, as mentioned above, these frequencies are determined mainly by a relative velocity

of the cylinder and the fluid: the latter remains constant with the flow velocity, again in order to keep the balance between the hydrodynamic forces and the weight of the cylinder. Also, f and f_f are both independent of the cylinder diameter: this result involves likely a compensation between different effects and will require $2D$ numerical simulations in order to be explained.

Further studies are needed to understand better the analogies and differences of these two types of instabilities as well as the weak dependence of variables like α on all the control parameters investigated (D/H, L/W). Regarding the fluttering instability, the characteristics of the fluid are important parameters to be investigated.

ACKNOWLEDGMENTS

We thank B. Semin for his careful reading of the manuscript and his useful comments and J.E. Wesfreid for useful suggestions. We acknowledge the RTRA Triangle de la Physique and the LIA PMF-FMF (Franco-Argentinian International Associated Laboratory in the Physics and Mechanics of Fluids). The work of one of us (VD) was supported by a Bernardo Houssay grant allocated by the Argentinian and French ministries of research.

REFERENCES

[1] A.B. Richou, A. Ambari, and J.K. Naciri, "Drag force on a circular cylinder midway between two parallel plates at very low Reynolds numbers. Part 1: Poiseuille flow (numerical)," Chem. Eng. Sci. **59**, 3215–3222 (2004).

[2] A. B. Richou, A. Ambari, M. Lebey, and J. K. Naciri, "Drag force on a cylinder midway between two parallel plates at $Re \ll 1$. Part 2: moving uniformly (numerical and experimental)," Chem. Eng. Sci. **60**, 2535–2543 (2005).

[3] B. Semin, J-P. Hulin and H. Auradou, "Influence of flow confinement on the drag force on a static cylinder," Phys. Fluids **21**, 103604 (2009).

[4] H. Faxén, "Forces exerted on a rigid cylinder in a viscous fluid between two parallel fixed planes," Proc. R. Swed. Acad. Eng. Sci. **187**, 1–13 (1946).

[5] A.S. Dvinsky and A.S Popel, "Motion of a rigid cylinder between parallel plates in Stokes flow. Part 1: motion in a quiescent fluid and sedimentation," Computers andFluids **15**, 391–404 (1987).

[6] A.S. Dvinsky and A.S Popel. 'Motion of a rigid cylinder between parallel plates in Stokes flow. Part 2: Poiseuille and Couette flow," Computers & Fluids **15**, 405–419 (1987).

[7] E. Eklund and A. Jernqvist, "The motion of a neutrally buoyant circular cylinder in bounded shear flows," Chem. Engng. Sci. **49**, 3765–3772 (1994).

[8] H.H. Hu, "Motion of a circular cylinder in a viscous liquid between parallel plates," Theoret. Comput. Fluid Dynamics **7**, 441–455 (1995).

[9] S. Camarri and F. Giannetti, "Effect of confinement on three-dimensional stability in the wake of a circular cylinder," J. Fluid Mech. **642**, 477-487 (2010).

[10] C.H.K. Williamson, "Vortex dynamics in the cylinder wake," Annu. Rev. Fluid. Mech. **28**, 477-539 (1996).

[11] C.H.K. Williamson and R. Govardhan, "A brief review of recent results in vortex-induced vibrations," J. Wind Eng. Ind. Aerodyn. **96**, 713–735 (2008).

[12] P. Ern, F. Risso, D. Fabre and J. Magnaudet, "Wake-induced oscillatory paths of bodies freely rising or falling in fluids," Ann. Rev. Fluid. Mech. **44**,97–121 (2012).

[13] P. Assemat, D. Fabre et J. Magnaudet, "The onset of unsteadiness of two-dimensional bodies falling or rising freely in a viscous fluid: a linear study." J. Fluid Mech. **690**, 173–202 (2012).

[14] Y. Tanabe and K. Kaneko, "Behavior of a falling paper," Phys. Rev. Lett. **73**, 1372–1375 (1994).

[15] A. Belmonte, H. Eisenberg and E. Moses, "From flutter to tumble, Inertial Drag and Froude Similarity in Falling Paper," Phys. Rev. Lett.**81**, 345–348 (1998).

[16] U. Pesavento and Z.J. Wang, "Falling paper: Navier-Stokes solutions, model of fluid forces, and center of mass elevation," Phys. Rev. Lett. **93**, 144501 (2004).

[17] B. Semin, A. Decoene, J.P. Hulin, M.L.M. Francois and H. Auradou, "New oscillatory instability of a confined cylinder in a flow below the vortex shedding threshold," J. Fluid Mech. **690**, 345–365 (2012).

[18] M.V. D'Angelo, J.P. Hulin and H. Auradou, "Oscillations and translation of a free cylinder in a viscous confined flow," Phys. Fluids **25**, 014102 (2013).

[19] M. Sahin and R. G. Owens, "A numerical investigation of wall effects up to high blockage ratios on two-dimensional flow past a confined circular cylinder," Phys. Fluids **16**, 1–25 (2004).

[20] H. Berthet, "Single and collective fiber dynamics in confined microflows", PhD thesis, Pierre and Marie Curie University (2012).